

Feldspar crystallization under magma-mixing conditions shown by cathodoluminescence and geochemical modelling – a case study from the Karkonosze pluton (SW Poland)

E. SLABY^{1,*} AND J. GÖTZE²

¹ Institute of Geochemistry, Mineralogy and Petrology, Warsaw University, Al. Żwirki i Wigury 93, 02-089 Warsaw, Poland

² Institute of Mineralogy, TU Bergakademie Freiberg, Brennhausgasse 14, D-09596 Freiberg, Germany

ABSTRACT

Feldspars from the Karkonosze pluton (SW Poland) display many features compatible with magma mixing. The mixing hypothesis has been tested using a geochemical mass balance law resulting in two possible paths of magma hybridization. Based on the results of the geochemical calculation, feldspar samples have been chosen along both mixing lines for cathodoluminescence (CL) investigation which was used as the main tool for the reconstruction of their crystallization path. Changes in the conditions of nucleation and crystallization of the feldspars as well as their movement within the magma chamber have been recognized due to different luminescence characteristics. These changes in the conditions of crystallization obtained by CL allow a precise determination of the genetic affinity of the samples to more mafic or more felsic environments.

The results of the present study proved CL to be a valuable tool for the study of crystal-growth morphologies in a dynamic, turbulent environment and also as a geochemical tool for the reconstruction of various petrogenetic mechanisms (e.g. magma hybridization). Accordingly, the combination of CL with geochemical modelling provides corresponding information about magma evolution in an open system.

KEYWORDS: cathodoluminescence, Karkonosze pluton, Poland, feldspar, magma mixing.

Introduction

MAGMA mixing/mingling implies physical and chemical interaction between melts, leading to obvious disequilibrium conditions. Disequilibrium influences the nucleation and growth rate of crystals. Hibbard (1981) recognized textures in mantled minerals, which result from growth in an un-equilibrated system. His idea has been further developed by many subsequent studies carried out especially on plagioclases from felsic rocks (e.g. Barbarin, 1990; Bussy, 1990; Wark and Stimac, 1992; Anderson and Eklund, 1994; Müller and Seltmann, 2002; Baxter and Feely, 2002; Grogan and Reavy, 2002). The evidence of magma

mixing/mingling is found, in particular, in granite bodies and can be observed over a range of scales, from whole pluton down to single crystals. The composition and growth morphology of igneous feldspars reflect certain changes in their crystallization environment. They can give a reliable record of the crystallization dynamics of the melt and its thermal and compositional turbulence (e.g. Anderson, 1984). The growth morphology is usually investigated by determining the optical properties of feldspars using polarizing microscopy (e.g. Hibbard, 1981, 1994; Baxter and Feely, 2002; Grogan and Reavy, 2002). Geochemical tools such as the electron microprobe technique also support the research on disequilibrium textures (e.g. Ginibre *et al.*, 2002). The growth of feldspars in a dynamic environment has also been studied experimentally (Wark and

* E-mail: E.Slaby@uw.edu.pl

DOI: 10.1180/0026461046840205

Stimac, 1992). In most cases, the research was focused on plagioclases as studies of K-feldspars are rare (Long and Luth, 1986; Vernon, 1986; Cox *et al.*, 1996; Waight *et al.*, 2000).

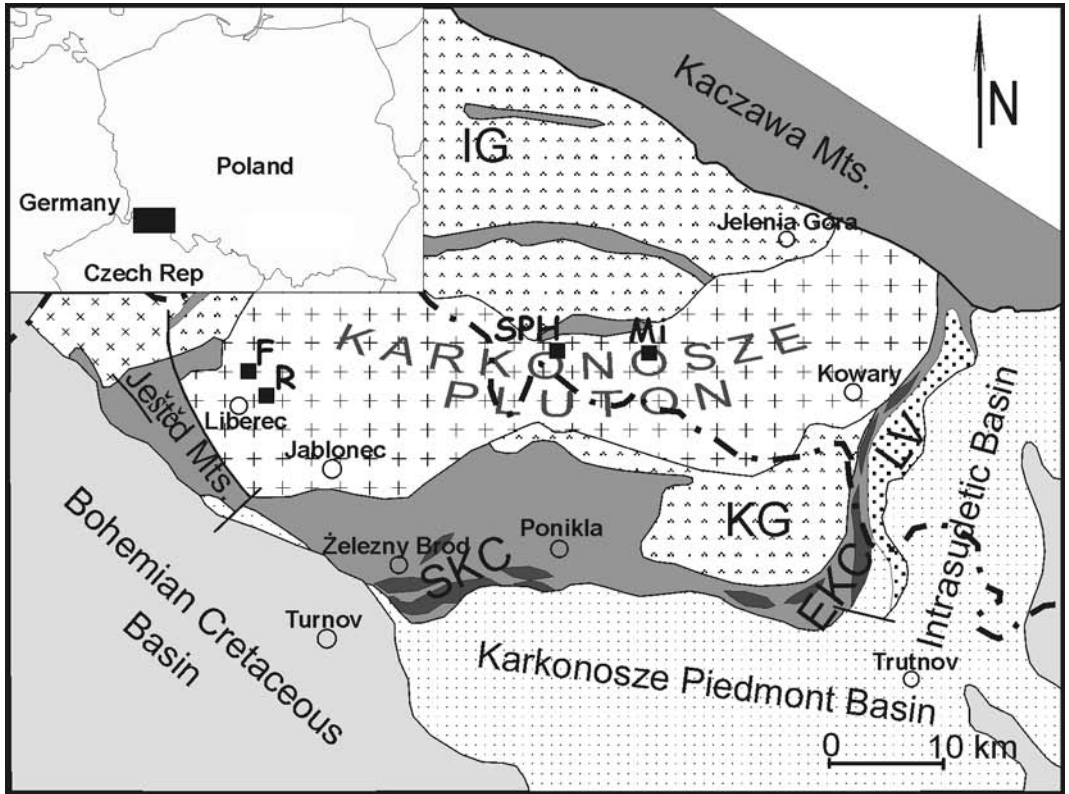
So far CL has been used only casually for the reconstruction of magma mixing/mingling processes. In actual fact, it appears to be highly suitable for the research of growth phenomena since many textures invisible in light microscopy are revealed by means of CL. In the present study we applied CL for the investigation of feldspar textures, proving its applicability for the reconstruction of the crystallization paths of feldspars under magma-mixing/mingling conditions. Furthermore, CL may provide information on the degree of magma hybridization. The luminescence of feldspar minerals is often very sensitive to such changes in the crystallization environment such as magma mixing. The trace elements incorporated in feldspars often reflect the chemical environment during their crystallization (e.g. Singer *et al.*, 1995; Tepley *et al.*, 2000; Ginibre *et al.*, 2002), and many of these elements are effective activators in feldspars (Mora and Ramseyer, 1992; Götze *et al.*, 2000). The element concentration necessary for luminescence activation can be very low, often below the detection limit of electron microprobe or other spatially resolved analytical techniques. Therefore, CL can be much more sensitive as a geochemical tool than many other analytical devices. The distribution of the trace elements and the changes in their concentration during hybridization should permit precise reconstruction of the space and time pattern of the process.

The identification and quantification of processes responsible for magma generation and evolution are realized by geochemical modelling (Rollinson, 1993). The behaviour of the elements is mostly considered in mass balance calculations. The mathematical approach to magma mixing processes shows the dependence between the degree of mixing, the composition of the melts involved in the mixing process and the composition of the hybridized melt (Rollinson, 1993; Martin, 2002).

Feldspars from the Karkonosze Massif (SW Poland) have been chosen for the present study. Rapakivi alkali feldspar megacrysts from the Karkonosze porphyritic granite are crystallized under magma mixing processes (Ślaby *et al.*, 2002). The combination of chemical analysis, CL and modelling was applied to obtain complex information about the entire crystallization process.

Geological setting

The Lower Carboniferous Karkonosze granite pluton belongs to the West Sudetes domain. It is located on both sides of the Polish-Czech border (Fig. 1). The domain is composed of a heterogeneous mosaic of pre-Permian basement fragments involved in the Variscides and is mostly considered a part of the Saxothuringian zone (e.g. Kossmat, 1927; Behr *et al.*, 1984; Franke *et al.*, 1993; Matte *et al.*, 1990; Matte, 1991). The pluton is mainly estimated as a late- (Wilamowski, 1998) or post-orogenic granite pluton (Diot *et al.*, 1994, 1995; Duthou *et al.*, 1991), although the mode of magma generation and emplacement is still a subject of debate (see Mierzejewski, 2002, for a review). The question concerning the composition of its protolith is one of the most interesting problems, as yet unresolved. The Karkonosze pluton consists of three texturally different granite facies: a coarse- to medium-grained porphyritic facies, a medium- to fine-grained (equigranular) facies and a granophyric facies (Borkowska, 1966). Due to different modal compositions, Klominsky (1969) distinguished four types of biotite granite within the pluton – a two-mica granite, and three types of granodiorite. Although several authors point to similar geochemical features of the whole pluton (Pin *et al.*, 1987, 1988; Duthou *et al.*, 1991), the existing data cannot be interpreted in a unique way, especially in the case of the porphyritic granite. The Rb/Sr data of samples from two quarries located close together show initial $^{87}\text{Sr}/^{86}\text{Sr} = \text{Sr}_i$ of 0.7066 and 0.7056, respectively, with an estimated εNd_i of -3.5 (Pin *et al.*, 1988; Duthou *et al.*, 1991). Based on these isotopic data, the authors assume fairly primitive protoliths for the Karkonosze granite. The low Sr_i value indicates either an intracrustal magma source for the granite pluton or the admixture of a more basic component to crustal melts. The lamprophyre veins within the pluton are considered as remnants of mantle material, whereas the reworked enclaves found in porphyritic granite are assumed to be remnants of an older basic intrusion assimilated by the granite magma. According to Kennan *et al.* (1999), the low Sr_i ratio excludes gneisses from the Sudetes as potential source material of the granitic magma. The Karkonosze granite, however, shows some features of both 'S'- and 'I'-type granites (Pin *et al.*, 1987; Wilamowski, 1998). Borkowska (1966) suggested different sources for the Karkonosze magma including












-  low-grade metasediments with subordinate metavolcanics
-  medium-grade metasediments and metagranitoids
-  low-grade metamorphosed volcano-sedimentary sequences with abundant bimodal metavolcanics
-  low- to medium-grade metamorphosed volcano-sedimentary sequences dominated by mafic rocks
-  Late Proterozoic and Cambria/Ordovician granitoids
-  Variscan granitoids
-  Carboniferous and Permian syn- and post-orogenic deposits
-  Mesozoic platform deposits
-  Polish - Czech border

FIG. 1. Simplified geological map of the Karkonosze-Izera massif (after Patočka *et al.*, 2000). IG – Izera gneisses and granito-gneisses with belts of mica schists; EKC – Eastern Karkonosze Complex; LV – Leszczyniec unit; SKC – Southern Karkonosze Complex; SPH – Szklarska Poręba Huta quarry; MI – Michałowice quarry; R – Rudolfov quarry; F – Fojtka quarry.

gneisses, amphibolites and other rocks of amphibolite facies.

A structural study by Mazur (1995) reveals that the magma was emplaced immediately after its generation and could be linked to the final deformation event of the West Sudetes, an extensional collapse. The direction of magma flow was defined by fluidal feldspar alignment (Cloos, 1925; Mierzejewski, 2002). Using the spatial arrangement of megacrysts within the porphyritic facies, Mierzejewski (2002) reconstructed funnel-like structures, which may represent the paths used by magma pulses. These results were confirmed by investigations of the magnetic lineation (Diot *et al.*, 1995). Lineation appears in both granite and its metamorphic envelope and points to the simultaneous emplacement and extensional deformation of the metamorphic rock. The emplacement may be partly correlated with the growth of a regional dome, which reoriented the previous ductile thrusting structures on the flanks of the dome (Aleksandrowski *et al.*, 1997).

Magma-mixing model

Textures formed by mixing/mingling of two melts – a mafic (probably derived from the mantle) and a felsic (crustal) one – can be easily identified within granodiorites (Fig. 2a) and porphyritic

granites (Table 1). The occurrences of granodiorites are mainly located within the Czech part of the pluton in the inoperative quarries of Fojtka (F) and Rudolfov (R) (Fig. 1). Several microdioritic, hybridized enclaves (Fig. 2b) accompanying the porphyritic granite in many places, represent relics of mafic magma blobs (Słaby, 2002). On the Harker diagrams, major and trace elements display good linear trends over a wide silica range – from granodiorites (including enclaves) to granites (line X'X'' in Fig. 3a, Table 1). A long linear trend is usually consistent with mixing (Rollinson, 1993). It also excludes fractional crystallization with unchanged cumulate composition over a large range of differentiation, which is unrealistic in natural systems. The linear trend is defined by all main and trace elements. In addition, for some oxides and elements such as P₂O₅, CaO, MgO, Sr and Ba, some points plot out of the main trend and define a secondary trend (line Y'Y'' in Fig. 3b, Table 1). This additional trend is formed by granodiorites from Fojtka and some enclave samples. It may result from the mechanical introduction of certain minerals (e.g. feldspars and apatite) into the melt mixture.

The geochemical mass-balance law:

$$C_m = X_A \cdot C_A + (1 - X_A) \cdot C_B$$

has been used for major and trace elements to test the mixing hypothesis (Rollinson, 1993; Martin,



FIG. 2. Typical features of rocks from the Karkonosze massif: (a) granodiorite from Rudolfov (R) showing evidence of mixing and mingling (the arrow points to an extraneous domain with mantled feldspars, en – enclave with mechanically introduced alkali feldspars); (b) granite from the Szklarska Poręba Huta (SPH) quarry with mafic, dilated enclave.

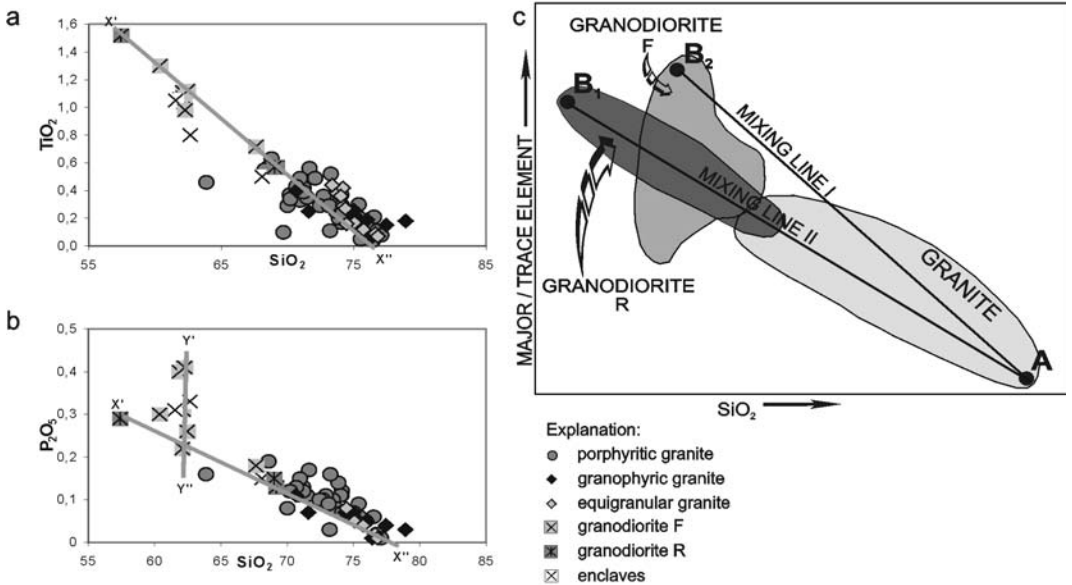


FIG. 3. Harker diagrams showing selected element plots of SiO_2 vs. TiO_2 (a), SiO_2 vs. P_2O_5 , (b) and two mixing models, and with different mixing lines (c) (see text for explanation).

2002) for several chosen poles from granodiorites and granites.

The symbols in the formula represent: Pole A – felsic magma; Pole B – mafic magma; C_A , C_B , C_M – concentration of one element in pole A, pole B and in the mixture, respectively; X_A , X_B – weight fraction of A and B in the mixture, where $X_A = (1 - X_B)$

Two possible pole selections are shown on the schematic plot in Fig. 3c. The granodiorites from Rudolfov (B_1 – mixing line I) or from Fojtka (B_2 – mixing line II) have been chosen as contaminants (mafic magma). The most silica-rich porphyritic granite from Szklarska Poręba Huta (SPH) has been selected as pole A (felsic magma). It is assumed that the average porphyritic granite (Table 1) in the tested hypothesis is the result of a mixing between the poles A and B. The calculations have been done for major and trace elements except Rb, which shows behaviour consistent with fractional crystallization (Słaby *et al.*, 2003). Both processes, fractional crystallization and mixing, controlled the magma evolution within the Karkonosze pluton.

The derived equation ($y = X_A x$, where $y = C_M - C_B$, $x = C_A - C_B$) for the mixing line (I) is $y = 0.85x - 0.05$ ($R^2 = 0.99$), for the line (II) $y = 0.68x - 1.7$ ($R^2 = 0.99$). Both results are

acceptable: the plots go through the origin and display very good values for R^2 . The correlation in both cases is much better for the major elements alone.

Field evidence (textures) together with the geochemical data support the hypothesis of mixing/mingling. The results of the calculations illustrate that mixing/mingling between two compositionally different magmas can be considered as the main process responsible for the formation of the porphyritic granite, and they also account for most of the geochemical features of these granite facies. Depending on the path, 15–32% of the mafic contaminant would have been needed to form the porphyritic granite facies in the Karkonosze pluton.

CL observations on feldspars

Feldspars from rocks with different silica content have been investigated. The feldspars form two generations in each sample: alkali feldspar megacrysts with plagioclase rims (rapakivi texture) and matrix crystals. Plagioclase megacrysts are rare. The feldspar samples have been selected from three different genetic populations along both mixing lines including granites, granodiorites and enclaves found in granites and granodiorites. The chemical composition of the

TABLE 1. Composition of the rocks from the Karkonosze pluton.

	enR (B ₂)	enSPH	g-diR	g-diF (B ₁)	g-di	g-di	grSPH (A)	gr	grMI	gr	Average**
SiO ₂	57.41	62.13	69.18	62.18	62.08	61.87	77.07	68.58	70.96	73.2	73.13
TiO ₂	1.52	1.07	0.57	1.04	1.11	1.06	0.08	0.57	0.49	0.11	0.29
Al ₂ O ₃	15.21	15.3	13.87	15.76	14.84	15.94	12.59	14.44	13.97	11.23	13.2
Fe ₂ O ₃ *	8.58	6.0	3.63	5.71	6.29	5.67	0.74	3.73	3.1	0.94	1.97
MnO	0.16	0.1	0.07	0.09	0.1	0.08	0.02	0.07	0.06	0.03	0.05
MgO	3.14	2.48	1.1	2.1	2.86	2.16	0.03	1.05	0.96	0.13	0.56
CaO	4.86	3.85	2.39	3.86	3.84	4.06	0.73	2.04	2.02	0.7	1.12
Na ₂ O	3.8	3.46	3.31	3.48	3.44	3.64	3.25	3.27	3.46	2.99	3.21
K ₂ O	3.04	3.43	4.2	3.39	3.46	3.41	4.95	4.52	3.63	4.64	4.64
P ₂ O ₅	0.29	0.31	0.13	0.41	0.22	0.4	0.01	0.19	0.15	0.03	0.09
Total	98.01	98.13	98.45	98.02	98.24	98.29	99.47	98.46	98.80	94.00	98.26
Cr	71	59.5	27	39	80	62	11	21	25	11	16
V	n.d.	83.5	n.d.	81	86	n.d.	7	42	35	8	22
Co	n.d.	19.5	n.d.	12	27	n.d.	0	0	0	0	3
Ni	n.d.	47.5	n.d.	35	60	n.d.	10	17	21	12	15
Cu	n.d.	8	n.d.	12	4	n.d.	0	0	0	0	0
Zn	111	81	52	87	75	83	6	62	51	26	33
Rb	142	173	134	158	188	145	190	224	199	301	249
Sr	253	246	237	273	219	286	17	166	153	30	86
Y	56	33	60	33	33	37	31	37	40	43	34
Zr	199	280	177	371	189	305	56	228	203	87	132
Nb	14	14.5	14	14	15	13	15	15	12	6	12
Ba	485	642.5	418	859	426	967	9	631	407	91	290
La	n.d.	22.5	n.d.	22	23	n.d.	0	41	14	17	18
Ce	n.d.	51.5	n.d.	66	37	n.d.	25	59	66	38	45
Pr	n.d.	6	n.d.	7	5	n.d.	2	6	5	5	4
Nd	n.d.	24.5	n.d.	27	22	n.d.	9	20	15	17	16
Sm	n.d.	5.5	n.d.	7	4	n.d.	3	4	3	2	4

*total Fe; ** average composition of porphyritic granite; en – enclave, g-di – granodiorite, gr – porphyritic granite; n.d. – not determined

feldspars was analysed by means of EMPA profiles. Quantitative point analyses of Si, Al, K, Na, Ca, Mn, Fe and Ba were performed in 10 µm steps across every feldspar grain selected for CL investigation. The chemical composition (without the concentrations of Fe and Mn) of selected feldspar crystals is presented in Table 2.

Feldspar megacrysts in granodiorite and granite

The common feature of alkali feldspar megacrysts in all cases (granite and granodiorite) is the rapakivi texture. Additionally, all megacrysts comprise many mineral inclusions, mainly of plagioclase, which usually occur along growth zones or are spread irregularly within the crystal. We tried to reconstruct the crystallization path of

the megacrysts from the two porphyritic granite quarries of Szklarska Poręba Huta (SPH) and Michałowice (MI). The composition of the MI granite is much more basic than that of the SPH granite, plotting into the centre of the mixing line II, whereas the SPH sample is compositionally close to pole A (the most evolved felsic melt) in both mixing lines. We have also chosen megacrysts from the Fojtká (F) granodiorite (contaminant B₂) and the Rudolfov (R) granodiorite for CL investigations.

The CL investigation reveals that megacrysts from SPH, MI and R have plagioclase inclusions of similar origin (Fig. 4*a,b*), although some differences are noticeable. A common feature of these plagioclase inclusions is a green luminescing core (An₃₃), surrounded by discordant zoning

TABLE 2. Electron microprobe analyses of feldspars from the Karkonosze pluton.

	enR		enSPH		g-diR		g-diF		grSPH		grSPH		grSPH		grMI		grMI		grMI		
	pl	pl	af-m	pl-rr	af-m	pl-rr	af-m	pl-rr	af-mc	pl-rr	af-ma	pl-inc	af-ma	pl-rr	af-mm	pl-rr	af-mc	pl-rr	af-ma	pl-inc	af-ma
SiO ₂	62.19	64.23	65.03	67.12	64.78	67.74	65.81	64.97	69.35	62.73	65.06	64.13	65.51	61.37	65.51	64.13	65.06	61.37	69.08	64.94	64.94
Al ₂ O ₃	23.71	21.76	18.51	20.57	18.20	21.07	18.54	18.45	20.61	23.50	18.60	18.52	18.40	23.79	18.40	18.52	18.60	23.79	19.22	18.43	18.43
CaO	4.76	2.19	0.01	1.09	0.00	1.86	0.00	0.03	1.03	5.05	0.00	0.00	0.00	5.37	0.00	0.00	0.00	5.37	0.79	0.00	0.00
Fe ₂ O ₃	0.35	0.00	0.08	0.02	0.01	0.29	0.11	0.03	0.04	0.00	0.17	0.10	0.04	0.11	0.04	0.10	0.17	0.11	0.02	0.01	0.01
BaO	0.03	0.00	0.38	0.02	0.62	0.07	0.91	0.14	0.00	0.00	0.11	1.56	0.17	0.07	0.17	1.56	0.11	0.07	0.00	0.00	0.00
Na ₂ O	8.84	8.24	0.58	10.90	0.28	10.35	0.61	0.19	10.34	8.60	0.23	0.46	0.42	8.60	0.42	0.46	0.23	8.60	11.12	0.73	0.73
K ₂ O	0.26	2.98	15.95	0.11	16.26	0.06	15.34	15.98	0.09	0.34	16.49	15.03	15.88	0.11	15.88	15.03	16.49	0.11	0.10	16.17	16.17
Total	100.14	99.40	100.54	99.83	100.15	101.44	101.32	99.79	101.46	100.22	100.66	99.80	100.42	99.42	100.42	99.80	100.66	99.42	100.33	100.28	100.28
Si	2.76	2.89	3.00	2.94	3.00	2.93	3.00	3.00	2.98	2.77	2.99	2.99	3.00	2.71	3.00	2.99	2.99	2.71	3.01	2.99	2.99
Al	1.24	1.45	1.00	1.06	0.99	1.07	1.00	1.00	1.04	1.22	1.01	1.02	1.00	1.29	1.00	1.02	1.01	1.29	0.98	1.00	1.00
Ca	0.23	0.10	0.00	0.51	0.00	0.09	0.00	0.00	0.05	0.24	0.00	0.00	0.00	0.30	0.00	0.00	0.00	0.30	0.04	0.00	0.00
Fe	0.01	0.00	0.00	0.00	0.00	0.01	0.00	0.00	0.00	0.00	0.00	0.00	0.00	0.00	0.00	0.00	0.00	0.00	0.00	0.00	0.00
Ba	0.00	0.00	0.01	0.00	0.01	0.00	0.02	0.00	0.00	0.00	0.00	0.00	0.00	0.00	0.00	0.00	0.00	0.00	0.00	0.00	0.00
Na	0.76	0.71	0.05	0.93	0.03	0.87	0.05	0.02	0.86	0.74	0.03	0.04	0.04	0.68	0.04	0.04	0.03	0.68	0.94	0.06	0.06
K	0.01	0.17	0.94	0.01	0.96	0.00	0.89	0.97	0.01	0.02	0.97	0.89	0.93	0.02	0.93	0.89	0.97	0.02	0.01	0.95	0.95

en – enclave, g-di – granodiorite, gr – porphyritic granite, pl – plagioclase, af – alkali feldspar, m – megacryst, c – core, mm – margin, rr – rapakivi rim, inc – inclusion, ma – matrix

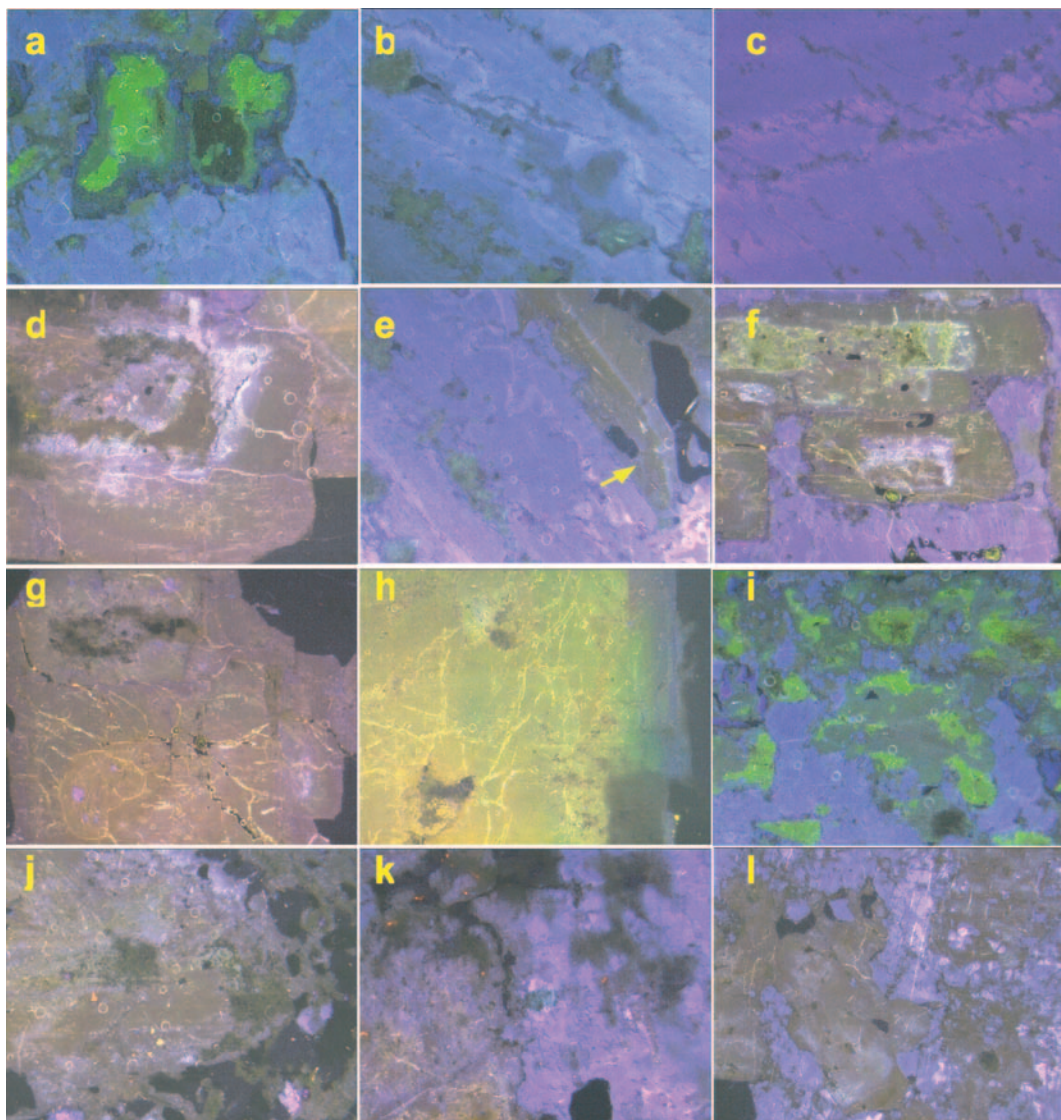


FIG. 4. CL images of alkali-feldspar megacrysts from granite and granodiorite, and matrix alkali feldspars (width of all micrographs is 1.6 mm). (a–b) inclusions of plagioclase in the core of megacrysts from the Szklarska Poręba Huta (a) and Rudolfov (b) quarries; (c) zoning in a K-feldspar megacryst from Rudolfov (R) (not discernible under cross-polarized light); (d–e) plagioclase rapakivi rims on K-feldspar megacrysts from Michałowice (d) and Rudolfov (e) (the arrow indicates the rim); (f) plagioclase inclusions in the marginal part of a megacryst from Michałowice; (g) glomerophytic plagioclase from the MI granite; (h) plagioclase rapakivi rim on a K-feldspar megacryst of a SPH sample; (i) plagioclase inclusions in the marginal part of a megacryst in a sample from Szklarska Poręba Huta; (j) plagioclase on the margin of the enclave in the granodiorite from Rudolfov; (k–l) marginal part (k) and core (l) of a megacryst in a sample from Fojtka.

and often displaying signs of multiple resorption ($An_{27-18-15}$). The intensity of the green luminescence decreases toward the edges of the crystal.

The blue luminescing rim (An_{5-1}) appears mostly in SPH (Fig. 4a) and MI (not shown) and usually gives the inclusion a euhedral habit. The rim

probably grew in equilibrium with the surrounding alkali feldspar. The green CL colour is caused by trace amounts of Mn^{2+} , which activate an emission band at ~ 565 nm (Götze *et al.*, 2000). We believe that the decreasing Mn concentration reflects primary crystallization conditions, since the dull green zone does not exhibit any feature of postmagmatic albitization (Leichmann *et al.*, 2003). Alteration of plagioclases (dark patches without luminescence) results in a mixture of secondary Ca-rich phases. The stages of dissolution and re-growth within the core of the plagioclase inclusions are clearly visible in SPH megacrysts (Fig. 4a). An apparent relation of plagioclase inclusions to dissolution and re-growth zones in alkali feldspar occurs in R megacrysts (Fig. 4b). All inclusions form irregular patches rather than well-shaped crystals and are mostly lacking the last, blue luminescing zone.

The growth process of R megacrysts appears to have been very dynamic. Feldspars show distinct zoning under CL because of variable densities of structural defects (Fig. 4c). Such differences in the luminescence emission characteristics can reflect variations in the crystallization environment and/or trace-element uptake during crystal growth (Götze *et al.*, 2000). The zoning appears only in megacrysts collected from granodioritic rocks, where, according to field evidence, magma mixing occurs.

The rapakivi rim on the megacrysts probably crystallized under conditions different from those of the plagioclase inclusions. The rims on megacrysts of MI and R samples seem to have a similar origin, since both exhibit the same pinkish luminescence (Fig. 4d,e). The MI rim is composed of plagioclase crystals that are attached to the megacryst (Fig. 4d). The textures of these rims show disequilibrium stages recorded by the resorbed core and the complex discordant zoning. The R plagioclases nucleated directly on the surface of megacrysts (see arrow in Fig. 4e) and show concordant growth zoning. Plagioclases on the edges of megacrysts also show mutual textures (Fig. 4f). A single plagioclase of glomerophytic habit, which shows a complex growth history including syneusis, was found within MI samples (Fig. 4g).

The rapakivi rims in SPH samples differ significantly from those in the MI and R samples. Plagioclases do not show pinkish luminescence, and no resorption textures could be revealed. Their growth proceeded in an almost

equilibrated system and is characterized by slight zoning with a continuous change of the luminescence colour from reddish-green to navy-blue (Fig. 4h). The change of the CL colour is caused by varying amounts of the defect centres of the type Fe^{3+} (red CL), Mn^{2+} (green CL) and/or $Al-O^- - Al$ (blue CL; Götze *et al.*, 2000) and may, therefore, also reflect changes in the redox conditions. Plagioclase inclusions at the edges of the SPH megacrysts (Fig. 4i) show similar luminescence characteristics to those from the core of the megacrysts.

Single plagioclase megacrysts have been found in R and SPH samples. Their luminescence is similar, fairly pinkish (Fig. 4j). The feldspars are usually dusty with gentle irregular, obscured zoning patterns.

Rapakivi megacrysts found in F granodiorites are different from the above-mentioned R, MI and SPH samples. The pinkish luminescence colours of both inner plagioclase inclusions and rapakivi rims of the F megacrysts (Fig. 4k,l) indicate similar crystallization conditions. The rim plagioclases do not show signs of heterogeneous nucleation on the alkali feldspar surface, however, their growth often has inward character. The cores of the plagioclases and the surrounding zones are heterogeneous as shown by different degrees of alteration (Fig. 4k). The plagioclase inclusions in the F megacryst also form patterns different from those found in the R, MI and SPH samples. They are rather poikilitic, non-uniformly luminescing plagioclases with K-feldspar inclusions, subsequently overgrown by K-feldspar megacrysts (Fig. 4l). They show gentle discordant zoning visible only under CL. The megacryst itself displays domain texture under CL, pointing to a dynamic magmatic environment. The textures reveal fluctuations during the crystallization process, compositional changes within the domains, resorption and regrowth. Similar fluctuations have been observed in the R samples. They are less common in SPH and MI megacrysts.

Matrix feldspars in granodiorite and granite

Blue to navy-blue luminescing matrix K-feldspars in F and R granodiorite display various growth patterns. The zoning is either irregular, discordant (Fig. 5a,b) or regular, concordant (Fig. 5c). The visible dull blue luminescence in the marginal part of the K-feldspar changes into light-blue in the core part. In particular the irregular pattern

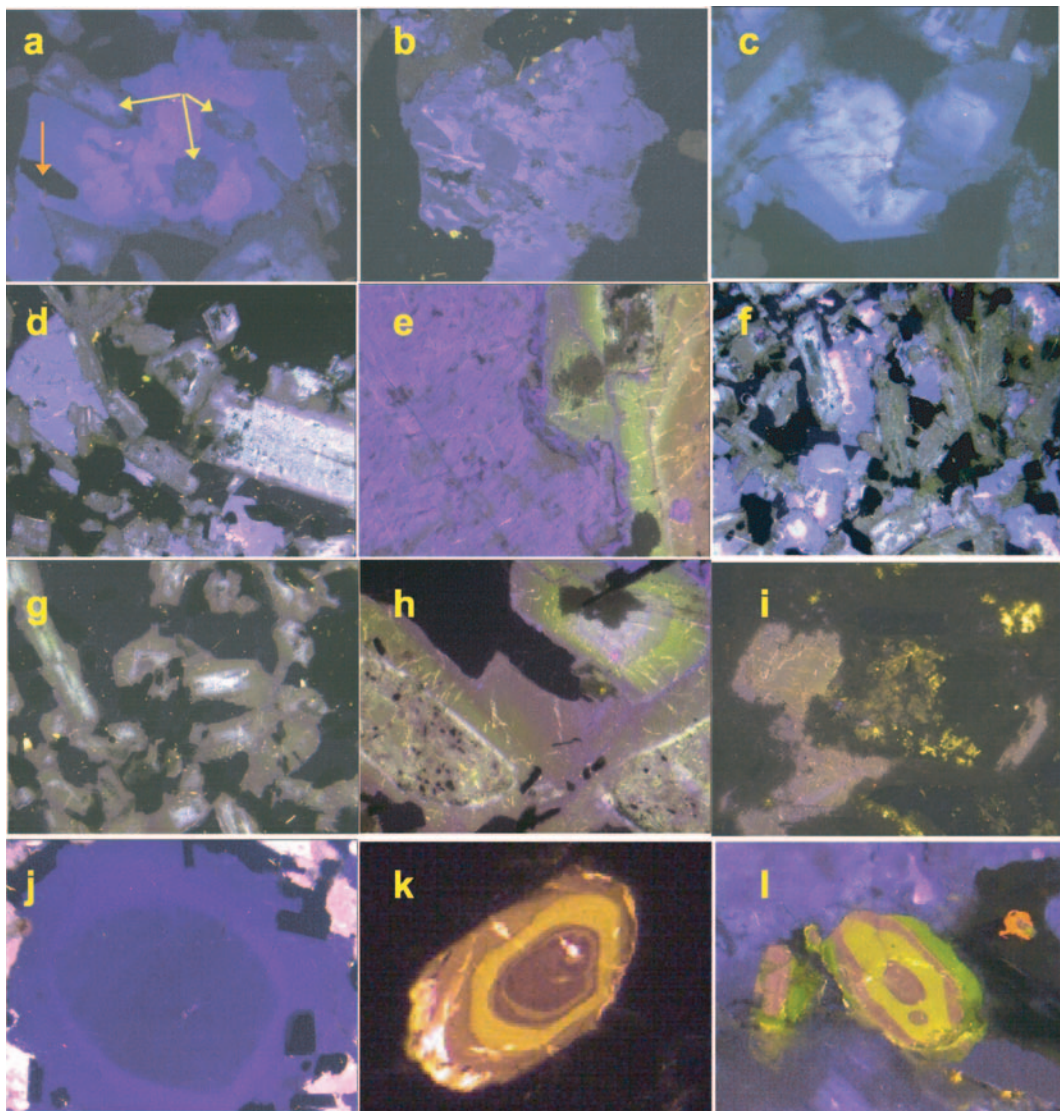


FIG. 5. CL images of matrix and enclave minerals in granodiorite and granite, respectively (width of micrographs for *a–f* is 1.6 mm, for *g–i* is 0.8 mm). (*a–c*) different zonation patterns in matrix alkali feldspars in the granodiorite from Fojtka (yellow arrows = plagioclases, orange arrow = apatite); (*d*) matrix plagioclase in the granodiorite from Fojtka; (*e*) blue luminescing matrix K-feldspar (left) with a plagioclase crystal (right) in the granite from Szklarska Poręba Huta close to the margin of the mafic enclave; (*f–g*) lath-shaped, zoned plagioclases from enclaves in the Rudolfov granodiorite (*f*) and the enclave from the Szklarska Poręba Huta granite (*g*); (*h*) distinctly zoned plagioclase crystals from the contact between enclave (lower part) and Szklarska Poręba Huta granite (upper right corner); (*i*) euhedral and interstitial plagioclase in the core part of the enclave within the Szklarska Poręba Huta granite showing strong alteration features; (*j*) zoned quartz crystal in the granodiorite from Fojtka; (*k–l*) strongly zoned apatite crystals in the granodiorite from Fojtka (*k*) and the granite from Michałowice (*l*) representing the variations in chemical composition.

points to dynamic, probably kinetically driven crystal growth in a fluctuating environment.

Matrix plagioclases in the F and R samples show luminescence zoning from bright pinkish-

blue in the core to dark pinkish at the rims (Fig. 5*d*), which is similar to the rapakivi rims around the megacrysts within granodiorites. Matrix K-feldspars from the granite are homogeneous, with dark-blue luminescence, whereas the matrix plagioclases resemble the rapakivi rims on K-feldspar megacrysts (Fig. 5*e*).

Feldspars from enclaves

Microdioritic enclaves, sometimes with mechanically introduced feldspars, have been found in R granodiorites as well as in SPH and MI granites (Fig. 2*a–b*). We took samples from enclaves with different modal composition. The enclave from the granodiorite (enR) comprises plagioclases and alkali feldspars, enclaves from granites, only plagioclases. The CL investigations revealed further differentiation criteria. The alkali feldspars from the R enclave show strong concordant or irregular zoning (Fig. 5*f*) similar to that found in the groundmass K-feldspar from the F and R granodiorites. The plagioclases luminesce brownish-pink (or pinkish-brown) and display zoning under CL. The zoning in some of the crystals has recurrent character (not shown in the figure) with a core zone of ternary feldspar composition (Table 2) and blue luminescence. The plagioclases from enclaves, irrespective of the place they have been collected, resemble matrix plagioclases from R and F samples. Some of the enclaves preserved in the granitic part of the pluton are very similar to those of the microdioritic composition found in R samples, but the alkali feldspars are lacking (Fig. 5*g*). Plagioclases in these samples are strongly concordantly or patchy zoned with generally brownish-pink luminescence. Those with patchy patterns possess ternary feldspar composition.

The enclaves exhibit various extents of hybridization. The timing of hybridization and re-equilibration is different in various individual samples. The CL was used to reconstruct the successive stages of both processes. Figure 5*h,i* presents feldspars from the edge and the central part of the microdioritic enclave found in the SPH quarry. In both images, fresh plagioclases crystallized in the voids of the enclave and filled out the space between the feldspars of the first generation. The void feldspars have been formed at the last stage of melt equilibration and crystallization. Their luminescence points to the same kind of activators as in the outer zone of plagioclases in granite (upper right corner of the “h” image) as

well as in the outer zone of both resorbed plagioclases belonging to the edge part of the enclave. The plagioclases from the enclave were apparently not in equilibrium with the melt. The equilibration of the system caused their alteration (Fig. 5*i*). The plagioclases on the edges of the enclave also show some stages of disequilibrium during their growth. They are clearly a product of the interaction of two melts.

CL observations on other minerals

Quartz phenocrysts, frequently mantled by ocellar biotite and hornblende, were found in the F and R granodiorites. In the other rocks, quartz occurs as groundmass crystals. Under CL it is distinctly zoned in the granodiorites (Fig. 5*j*) and homogeneous in granites. The growth zoning may be interpreted as resulting from rapid changes in Ti concentration in melt during the quartz growth and related variations in defect density in the crystals (Van den Kerkhof *et al.*, 1996; Müller *et al.*, 2000; Müller *et al.*, 2002).

Equant and acicular apatites frequently accompany granodiorite and granite parageneses. Feldspars and biotites are interlaced with acicular crystals. Larger equant apatite crystals show distinct growth zoning under CL pointing to at least three compositionally different crystallization environments (Fig. 5*k,l*). The change of the melt composition displays pulsating character resulting in the same luminescence of the core and some outer zones. The blue-violet luminescing zones can probably be related to more alkaline conditions, which favour the incorporation of *REE*, whereas the Mn²⁺ activated greenish-yellow CL points to a more acidic environment (e.g. Kempe and Götze, 2002). The effect of the repeated change in melt composition is detectable in both granodiorites and granites.

Discussion

The disequilibrium textures observed in feldspar megacrysts of the Karkonosze pluton, their chemical composition (especially trace element patterns) and the thermal history of their crystallization point to magma mixing processes (Słaby *et al.*, 2002; Słaby and Galbarczyk-Gąsiorowska, 2002). In addition, the low content of some of the trace elements in the system precludes the possibility of buffering their concentrations during fractional crystallization along the enR-SPH (B₁-A) or F-SPH (B₂-A) path (Słaby *et al.*,

2003). However, the chemical composition of the feldspars alone, even if combined with textural features, does not provide a precise determination of the mineral crystallization path. It is neither possible to reconstruct and compare similarities in the nucleation conditions of the crystals, nor to discriminate between feldspars growing *in situ* and those transported to their final location through processes operating within the magma chamber. Cathodoluminescence is a suitable tool for the identification of many of these growth features. The CL images obtained for the Karkonosze feldspars support the mixing hypothesis, but simultaneously also give abundant information about many of the discontinuities during magma evolution.

The SPH, MI, R and F megacrysts show a few discrete stages of changes in melt composition during crystallization. This raises a number of questions. The first refers to the location of nucleation of megacrysts. Did the nucleation take place in a felsic or in a hybridized melt, and in the latter case in one showing more affinity to mafic

or felsic composition? The similarities and differences are summarized in Figs 6 and 7. In view of the similar luminescence characteristics of plagioclase inclusions, the core parts of megacrysts from the R granodiorite and both granites (SPH and MI) seem to be of a common origin. The megacrysts nucleated and grew in a similar environment, although they originate from three compositionally different points in the middle and at the very end of the mixing line (see for comparison Fig. 3 – mixing line II). The CL images clearly reveal differences in the crystallization dynamics for various parts of the K megacrysts as well as the lack of equilibrium conditions at many stages during their formation. The CL images of plagioclase inclusions from the R, SPH and MI megacrysts also reveal different growth timings. Although the process terminated earlier in the R megacrysts, it was much more dynamic than in the SPH and MI samples. The crystallization path starts to differentiate in the marginal part of the megacrysts (variable luminescence of the plagioclase inclusions)

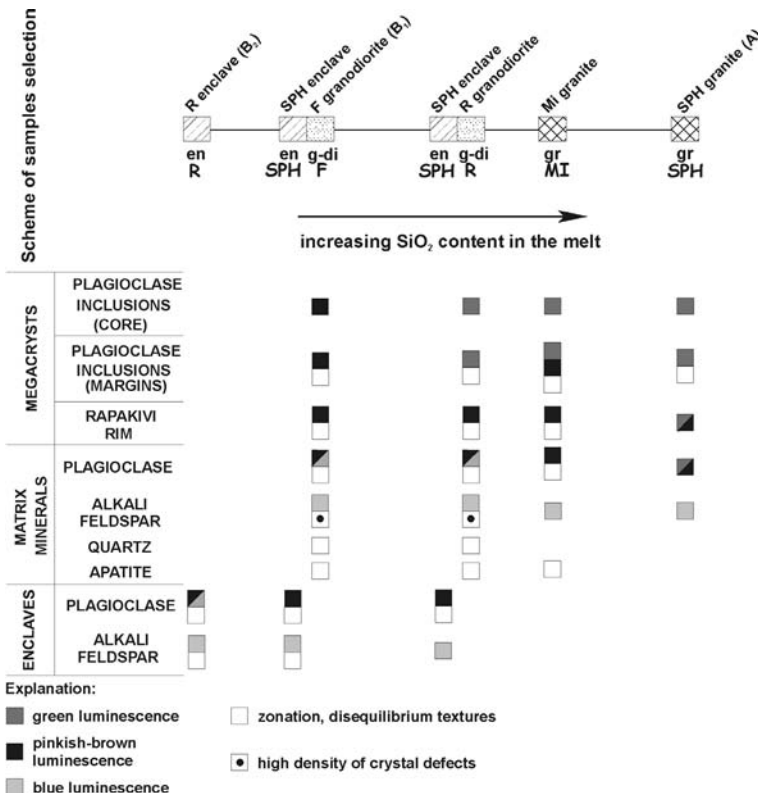


Fig. 6. Summary sheet of the CL data concerning the crystallization environment of the Karkonosze feldspars.

showing the biggest difference in the development of rapakivi rims. The CL characteristics for the rapakivi rims in R and MI plagioclases are similar, but the nucleation and growth process are different. The MI megacrysts, taken from the middle part of the mixing line ($X_A \approx 0.25$), recorded some additional events of disequilibrium growth compared with the R samples. The rapakivi rims on SPH megacrysts (from the granite compositionally close to the A pole) were formed without interruption of the growth process.

Looking at both mixing lines, there is a notable difference in the development of megacrysts in the granodioritic R and F samples. On the other hand, F and MI megacrysts show similarities in the development of the rapakivi rim, which is different from the core part. The marginal parts of all the samples were formed under conditions close to equilibrium and in an environment compositionally similar to F and MI samples.

Considering the development of feldspars in the F samples it is unclear whether some of the F megacrysts are mechanically added to the system or not. The trend 'Y'Y'' (Fig. 3b) could indicate such a possibility for both plagioclases and K-feldspars, whereas geochemical data preclude such a conclusion for the feldspar megacrysts from R samples. The results of the CL

investigations bring arguments, which could be interpreted in favour of the mechanical input of plagioclases in F samples and against the hypothesis of an addition of K-feldspar megacrysts. According to these data, alkali feldspar could nucleate in all of the investigated samples, the more mafic and the more felsic ones and no additional mechanical processes have to be taken into account.

In contrast to the alkali feldspar megacrysts in F samples, those from the other items show common features of nucleation and, generally, their growth corresponds to places along the mixing line. In conclusion, the CL data would place the nucleation process of megacrysts into a fairly intermediate environment that represents a hybridized melt. This conclusion is supported by the patterns of trace-element concentrations along megacrysts from granodioritic and granitic samples. The cores of all megacrysts are enriched in Ba and the pattern changes towards the edges of the crystals. Whereas megacrysts from granodioritic rocks usually preserve high Ba concentrations, those from granites show a step-wise change with a considerable decrease in Ba contents towards the marginal part (Słaby *et al.*, 2002; Słaby and Galbarczyk-Gąsiorowska, 2002). The Ba concentration is lower in granite samples than in granodiorites (Table 1). The trace element

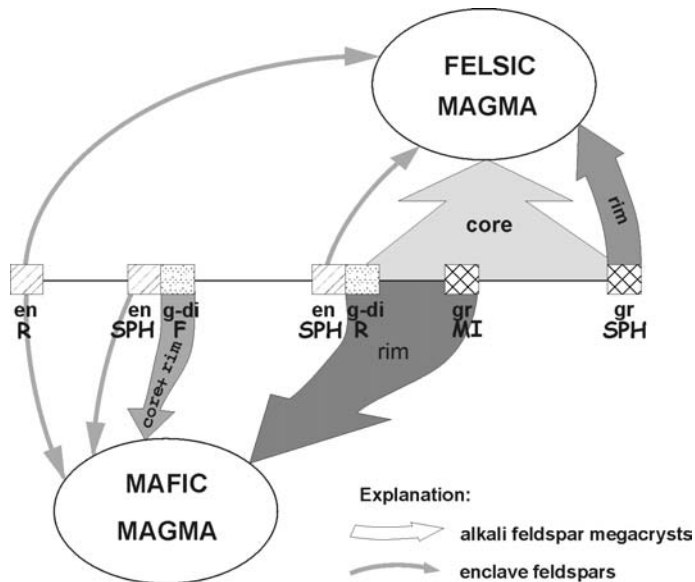


FIG. 7. Schematic sketch showing the genetic affinity of the Karkonosze feldspars to mafic or felsic environment revealed by CL.

distribution in granodioritic megacrysts is more homogeneous, which would suggest only minor variations of the crystallization conditions. At the same time, the granodioritic megacrysts display significant variations of structural defect patterns under CL, which could point to substantial differences of kinetic conditions in the crystallization environment. Their growth might have been repeatedly interrupted and continued due to periodic replenishment of the system with hybridized melt.

This conclusion is supported by the fact that matrix minerals in the samples occurring close to the mafic pole show periodic growth zoning, whereas the same minerals in granites display homogenous luminescence patterns. The dull-blue luminescence, which occurs alternately with the light-blue one in the groundmass K-feldspar, might reflect a more mafic input into the hybridized system. The crystallization environment of the matrix minerals in the granodiorites may be correlated with the growth of mineral inclusions in megacrysts of R, MI and SPH samples. The growth was interrupted and recommenced many times. The intensity of fluctuations during the magmatic crystallization, reflected by the density of crystal defects or the frequency of disequilibrium textures, decreases from a more mafic/intermediate environment to a more felsic one along the mixing line.

The same phenomenon is recorded in quartz crystals with an alternate transition from Ti-rich (more mafic) to Ti-poor (more felsic) environment. On the contrary, the growth process of megacrysts found in granites could be correlated with an increasing felsic component in the crystallization system. This might imply crystal transport within the chamber or a replenishment of the magma chamber with felsic melt.

The moment of the transition of a crystal to another environment can be precisely determined taking into account the CL characteristics of plagioclase inclusions. The event took place shortly before the formation of the rapakivi texture. The megacrysts of both alkali feldspar and plagioclases as well as single plagioclase crystals of glomerophytic habit represent a complex crystallization path. Some of their parts did not fit into the environment in which they were inherited and continued to grow. These features are clearly visible especially in the growth morphology of the plagioclases (compare the upper and lower left part of the plagioclase with the lower right part in the Fig. 4g).

Syneusis indicates a significant melt turbulence during the crystallization of feldspars (Vance, 1965, 1969). As per the observations of Grogan and Reavy (2002), syneusis appears among crystals of an earlier generation and is not found within matrix plagioclases. It is, in general, found within the granite samples from Karkonosze and usually accompanies crystals with complex disequilibrium textures. However, the crystals involved in syneusis show affinity to a more mafic environment. Accordingly, their presence in felsic items implies mechanical transport. The CL investigations clearly indicate intensive crystal transport within the magma chamber or during magma ascent. The idea of crystal transport by separated magma pulses is supported by a structural study on feldspar megacrysts from Karkonosze (Mierzejewski, 2002).

Apart from the question of whether some of crystals are mechanically added to compositionally more mafic or more felsic items, another question arises. It is not clear whether some of the core parts of the feldspar megacrysts are restites or not. The interpretation as restites is supported by the fact that those parts clearly differ from the surrounding rock and also from any other investigated rock of the Karkonosze pluton. The model of Huppert and Sparks (1988) predicts simultaneous melting and crystallization, accompanied by a lack of total restite resorption during the interaction of mafic magma with continental crust. Similarly, Klötzli *et al.* (2001) found domains of different isotopic composition in alkali feldspar megacrysts, which they interpreted as restite.

A further argument in favour of melt mixing is the similar microstructure of enclaves within both granodiorites and granites, which reflects igneous origin. The enclaves have been incorporated as magma blobs into the chamber. Their modal composition rules out the interpretation as cumulates. Plagioclases in all enclaves are euhedral, of elongated shape and zoned. They show high nucleation and slow growth rates. Needles of apatite (acicular habit) appear frequently within the feldspars and biotite. Some K-feldspar and plagioclase megacrysts are mechanically incorporated into the enclaves. All these features indicate their magmatic crystallization under strong undercooling (Didier, 1973; Vernon, 1983, 1990, 1991; Barbarin, 1990). Euhedral plagioclases in the enclaves often show ternary composition. The authors consider the zones of ternary feldspar composition, in the

present study usually of irregular shape, to be a result of hybridization. The zones occur more frequently in enclaves introduced into a melt distinctly enriched in silica. On the contrary, K-feldspar-bearing enclaves from more mafic items are depleted in plagioclases with clear ternary composition. The CL data brought strong arguments for a common origin of all of the enclaves. The CL characteristics of feldspars from enclaves collected from both granite and granodiorite are similar, indicating similar magma blob composition irrespective of the place of their incorporation into the chamber. The enclaves show various degrees of hybridization depending on the place of their incorporation. No clear evidence for late, interstitial melt segregation was found. Interstitial melt was found in some of the enclaves, however, displaying affinity with the granitic melt. This melt seems to be introduced into the enclave and then segregated within it. 'Bleeding' zones enriched in quartz and K-feldspars surround those enclaves. The zones are considered a typical feature of interstitial melt segregation (Vernon, 1991).

Conclusions

The CL investigations provided extremely valuable information about melt generation and evolution. The present study illustrates that CL enables us to identify differences in the geochemistry and dynamics of the environment during feldspar crystallization. It also provides additional information about the timing of feldspar formation. However, CL investigations are only very useful in combination with other analytical tools. Geochemical modelling, in particular, is needed before the CL work in order to define plausible petrogenetic mechanisms of magma differentiation.

In the present study, CL permitted the reconstruction of the crystallization path of feldspars and confirmed that the path found is common for many megacrysts from various samples of the Karkonosze pluton. Additionally, CL revealed a similar environment for plagioclase crystallization in enclaves, granodiorites and partly in rapakivi rims of some of the megacrysts found in granites. The affinity with so many igneous environments can be explained by the common origin of the rocks, which can be interpreted as compatible with magma mixing. The crystallization environment displays either affinity with more mafic or felsic composition

depending on the periodic recharge of the magma chamber. This twofold behaviour of the affinity in the crystallization path is shown in Fig. 7.

The CL observations were preceded by the identification of the main process responsible for magma differentiation, i.e. magma mixing/mingling by means of geochemical modelling. In the presented mixing models two means of feldspar nucleation and growth are suggested. Comparing the CL data with those from the modelling we conclude that the most likely path of feldspar formation in the Karkonosze pluton includes the contamination of a felsic melt with a mafic one of B₂ composition (enclave from Rudolfov). However, the other path, including F granodiorites as contaminant, cannot definitely be excluded and could also contribute to the formation of some of the megacrysts.

Acknowledgements

We would like to acknowledge helpful discussions concerning geochemical modelling with H. Martin, A. Finch and A. Mueller, whose comments are appreciated. We also wish to thank A. Dobrowolska for drawing all the figures.

References

- Aleksandrowski, P., Kryza, R., Mazur, S. and Źaba, J. (1997) Kinematic data on major Variscan strike-slip faults and shear zones in the Polish Sudetes, northeast Bohemian Massif. *Geological Magazine*, **133**, 727–739.
- Anderson, A.T. (1984) Probable relation between plagioclase zoning and magma dynamics, Fuego Volcano, Guatemala. *American Mineralogist*, **69**, 660–676.
- Anderson, A.T., Jr. and Eklund, O. (1994) Cellular plagioclase intergrowths as a result of crystal magma mixing in the Proterozoic and Aland rapakivi batholith, SW Finland. *Contributions to Mineralogy and Petrology*, **117**, 124–136.
- Barbarin, B. (1990) Plagioclase xenocrysts and mafic magmatic enclaves in some granitoids of the Sierra Nevada batholith, California. *Journal of Geophysical Research*, **95**, 17747–17756.
- Baxter, S. and Feely, M. (2002) Magma mixing and mingling textures in granitoids: examples from the Galway Granite, Connemara, Ireland. *Mineralogy and Petrology*, **76**, 63–74.
- Behr, H.J., Engel, W., Franke, W., Giese, P. and Weber, K. (1984) The Variscan belt in central Europe: main structures, geodynamic implications, open questions. *Tectonophysics*, **109**, 15–40.

- Borkowska, M. (1966) Petrography of Karkonosze granite. *Geologia Sudetica*, **II**, 7–119 (in Polish).
- Bussy, F. (1990) The rapakivi texture of feldspars in a plutonic mixing environment: a dissolution-recrystallization process? *Geological Journal*, **25**, 319–324.
- Cloos, H. (1925) Einführung in die tektonische Behandlung magmatischer Erscheinungen (Granittektonik). I Spez. Teil. *Das Riesengebirge in Schlesien*, 1–194.
- Cox, R.A., Dempster, T.J., Bell, B.R. and Rogers, G. (1996) Crystallization of the Shap granite: evidence from zoned K-feldspar megacrysts. *Journal of the Geological Society*, **153**, 625–635.
- Didier, J. (1973) *Granites and their Enclaves: The Bearing of Enclaves on the Origin of Granites*. Developments in Petrology, **3**. Elsevier, Amsterdam, 393 pp.
- Diot, H., Mazur, S. and Couturie, J.P. (1994) Magmatic structures in the Karkonosze granite and their relation to tectonic structures in the eastern metamorphic cover. *Igneous Activity and Metamorphic Evolution of the Sudetes Area*, Wrocław. Abstracts, pp. 36–39.
- Diot, H., Mazur, S. and Pin, C. (1995) Karkonosze batholith (NE Bohemian Massif): The evidence for pluton emplacement during transtensional-extensional collapse. *Journal of the Czech Geological Society*, **40**, 62.
- Duthou, J.L., Couturie, J.P., Mierzejewski, M.P. and Pin, C. (1991) Rb/Sr age of the Karkonosze granite on the base of the whole rock method. *Przegląd Geologiczny*, **2**, 75–79 (in Polish).
- Franke, W., Żelaźniewicz, A., Porębski, S.J. and Wajsprych, B. (1993) Saxothuringian zone in Germany and Poland: differences and common features. *Geologische Rundschau*, **82**, 583–599.
- Ginibre, C., Wörner, G. and Kronz, A. (2002) Minor and trace-element zoning in plagioclase: implications for magma chamber processes at Parímacota volcano, northern Chile. *Contributions to Mineralogy and Petrology*, **143**, 300–315.
- Götze, J., Krbetschek, M.R., Habermann, D. and Wolf, D. (2000) High-resolution cathodoluminescence of feldspar minerals. Pp. 245–270 in: *Cathodoluminescence in Geosciences* (M. Pagel, V. Barbin, Ph. Blanc and D. Ohnenstetter, editors). Springer-Verlag, Berlin, Heidelberg, New York, Tokyo.
- Grogan, S.E. and Reavy, R.J. (2002) Disequilibrium textures in the Leinster Granite Complex, SE Ireland: evidence for acid-acid magma mixing. *Mineralogical Magazine*, **66**, 929–939.
- Hibbard, M.J. (1981) The magma mixing origin of mantled feldspar. *Contributions to Mineralogy and Petrology*, **76**, 158–170.
- Hibbard, M.J. (1994) Mixed magma rocks. Pp. 242–260 in: *Petrography to Petrogenesis*, pp. 242–260. Prentice-Hall, New Jersey, USA.
- Huppert, H.E. and Sparks, R.S.J. (1988) The generation of granitic magmas by intrusion of basalt into continental crust. *Journal of Petrology*, **29**, 599–624.
- Kempe, U. and Götze, J. (2002) Cathodoluminescence (CL) behaviour and crystal chemistry of apatite from rare-metal deposits. *Mineralogical Magazine*, **66**, 135–156.
- Kennan, P.S., Dziedzic, H., Lorenc, M.W. and Mierzejewski, M.P. (1999) A review of Rb-Sr isotope patterns in the Carboniferous granitoids of the Sudetes in SW Poland. *Geologia Sudetica*, **32**, 49–53.
- Klominsky, J. (1969) Krkonosko-jizersky granitoid masif. *Sbornik Geologických Ved, Geologie*, **15**, 7–132 (in Czech).
- Klötzli, U.S., Koller, F., Scharbert, S. and Höck, V. (2001) Cadomian lower-crustal contributions to Variscan granite petrogenesis (South Bohemian Pluton, Austria). Constraints from zircon topology and geochronology, whole rock, and feldspar Pb-Sr isotope systematics. *Journal of Petrology*, **42**, 1621–1642.
- Kossmat, F. (1927) Gliederung des varistischen Gebirgsbaues. *Abhandlungen Sächsischen Geologischen Landesamts*, **1**, 1–39.
- Leichmann, J., Broska, I. and Zachovalova, K. (2003) Low-grade alteration of feldspar minerals: a CL study. *Terra Nova*, **15**, 104–108.
- Long, P.E. and Luth, W.C. (1986) Origin of K-feldspar megacrysts in granitic rocks: Implication of a partitioning model for barium. *American Mineralogist*, **71**, 367–375.
- Martin, H. (2002) Geochemical tools for modelling petrogenetic mechanisms. *Socrates-Erasmus Course, Warsaw*, pp. 1–80 (unpublished).
- Matte, P. (1991) Accretionary history and crustal evolution of the Variscan Belt in Western Europe. *Tectonophysics*, **196**, 309–337.
- Matte, P., Maluski, H., Rajlich, P. and Franke, W. (1990) Terrane boundaries in the Bohemian Massif: results of large-scale Variscan shearing. *Tectonophysics*, **177**, 151–170.
- Mazur, S. (1995) Structural and metamorphic evolution of the country rocks at the eastern contact of the Karkonosze granite in the southern Rudawy Janowickie Mts and Lasocki Ridge. *Geologia Sudetica*, **29**, 31–98.
- Mierzejewski, M.P. (2002) Additional data and remarks to Hans Cloos's work in Karkonosze Mts (Riesengebirge). *Zeitschrift für Geologische Wissenschaften*, **30**, 37–48.
- Mora, C.I. and Ramseyer, K. (1992) Cathodoluminescence of coexisting plagioclases, Boehls Butte

- anorthosite: CL activators and fluid flow paths. *American Mineralogist*, **77**, 1258–1265.
- Müller, A. and Seltmann, R. (2002) Plagioclase-mantled K-feldspar in the Carboniferous porphyritic microgranite of Altenberg-Frauenstein, eastern Erzgebirge/Krusne Hory. *Bulletin of the Geological Society of Finland*, **74**, 53–78.
- Müller, A., Seltmann, R. and Behr, H.-J. (2000) Application of cathodoluminescence to magmatic quartz in a tin granite – case study from the Schellerhau Granite Complex, Eastern Erzgebirge, Germany. *Mineralium Deposita*, **35**, 169–189.
- Müller, A., Kronz, A. and Breiter, K. (2002) Trace elements and growth patterns in quartz: a fingerprint of the evolution of the subvolcanic Podlesí Granite System (Krusne Hory, Czech Republic). *Bulletin of the Czech Geological Survey*, **77/2**, 135–145.
- Patočka, F., Fajst, M. and Kachlik, V. (2000) Mafic-felsic to mafic-ultramafic Early Palaeozoic magmatism of the West Sudetes (NE Bohemian Massif): the South Krkonose complex. *Zeitschrift Geologischen Wissenschaften*, **28**, 177–210.
- Pin, C., Mierzejewski, M.P. and Duthou, J.L. (1987) Isochronous age Rb/Sr of Karkonosze granite from the quarry Szklarska Poręba Huta and significance of initial ratio $^{87}\text{Sr}/^{86}\text{Sr}$ in this granite. *Przegląd Geologiczny*, **35**, 512–516.
- Pin, C., Mierzejewski, M.P., Duthou, J.L. and Couturie, J.P. (1988) Etude isotopique Rb-Sr du granite du Karkonosze. Pp. 43–47 in: *Petrologie et géologie du socle Varisque des Sudetes Polonaises: resultants de la co-operation entre les Universites de Wroclaw et Clermont-Ferrand* (S. Lorenc and A. Majerowicz editors). Universite de Wroclaw.
- Rollinson, H. (1993) *Using Geochemical Data: Evaluation, Presentation, Interpretation*. Longman, London, 352 pp.
- Singer, B.S., Dungan, M.A. and Layne, G.D. (1995) Textures and Sr, Ba, Mg, Fe, K and Ti compositional profiles in volcanic plagioclase: clues to the dynamics of calc-alkaline magma chambers. *American Mineralogist*, **80**, 776–798.
- Slaby, E. (2002) Porphyritic granite facies – Szklarska Poręba Huta. *Mineralogical Society of Poland Special Papers*, **20**, 245–247.
- Slaby, E. and Galbarczyk-Gąsiorowska, L. (2002) Barium in alkali feldspar megacrysts from Szklarska Poręba Huta porphyritic granite – possible indicator of magma mixing. *Mineralogical Society of Poland Special Papers*, **20**, 198–201.
- Slaby, E., Galbarczyk-Gąsiorowska, L. and Baszkiewicz, A. (2002) Mantled alkali-feldspar megacrysts from the marginal part of the Karkonosze granitoid massif (SW Poland). *Acta Geologica Polonica*, **52**, 501–519.
- Slaby, E., Wilamowski, A. and Gunia, P. (2003) Disimilar barium and rubidium behavior in Karkonosze porphyritic granite facies – mixing or fractional crystallization. *Mineralogical Society of Poland Special Papers*, **22**, 207–211.
- Tepley, F.J., III, Davidson, J.P., Tilling, R.I. and Arth, J.G. (2000) Magma mixing, recharge and eruption histories recorded in plagioclase phenocrysts from El Chichon Volcano, Mexico. *Journal of Petrology*, **41**, 1397–1411.
- Van den Kerkhof, A.M., Scherer, T. and Riganti, A. (1996) Cathodoluminescence and EPR analysis of Archean quartzites from the Nondweni Greenstone Belt, South Africa. *SLMS International Conference on Cathodoluminescence, Nancy*, abstracts p. 75.
- Vance, J.A. (1965) Zoning in igneous plagioclase: patchy zoning. *Journal of Geology*, **73**, 636–651.
- Vance, J.A. (1969) On syneusis. *Contributions to Mineralogy and Petrology*, **24**, 7–29.
- Vernon, R.H. (1983) Restite, xenoliths and microgranitoid enclaves in granites. *Journal of the Proceedings of the Royal Society of New South Wales*, **116**, 77–103.
- Vernon, R.H. (1986) K-feldspar megacrysts in granites – Phenocrysts, not porphyroblasts. *Earth Science Reviews*, **23**, 1–63.
- Vernon, R.H. (1990) Crystallization and hybridism in microgranitoid enclave magmas: microstructural evidence. *Journal of Geophysical Research*, **95**, 17849–17859.
- Vernon, R.H. (1991) Interpretation of microstructures of microgranitoid enclaves. Pp. 277–291 in: *Enclaves and Granite Petrology* (J. Didier and B. Barbarin, editors). Developments in Petrology, **13**. Elsevier, Amsterdam.
- Waight, T.E., Maas, R. and Nicholls, I.A. (2000) Fingerprinting feldspar phenocrysts using crystal isotopic composition stratigraphy: implications for crystal transfer and magma mingling in S-type granites. *Contributions to Mineralogy and Petrology*, **139**, 227–239.
- Wark, D.A. and Stimac, J.A. (1992) Origin of mantled (rapakivi) feldspars: experimental evidence of a dissolution- and diffusion-controlled mechanism. *Contributions to Mineralogy and Petrology*, **111**, 345–361.
- Wilamowski, A. (1998) Geotectonic environment of the Karkonosze and Tatra granite intrusions based on geochemical data. *Archiwum Mineralogiczne*, **LI**, 261–271 (in Polish).

[Manuscript received 25 April 2004:
revised 22 June 2004]